The Physiological Properties of a Novel Family of VDAC-Like Proteins from *Drosophila melanogaster*

Alexander G. Komarov,*‡ Brett H. Graham,† William J. Craigen,† and Marco Colombini*
*Department of Biology, University of Maryland, College Park, Maryland 20742; †Departments of Molecular and Human Genetics and Pediatrics, Baylor College of Medicine, Houston, Texas 77030; and ‡St. Petersburg Nuclear Physics Institute, Gatchina, Russia, 188350

ABSTRACT VDAC, a major protein of the mitochondrial outer membrane, forms voltage-dependent, anion-selective channels permeable to most metabolites. Although multiple isoforms of VDAC have been found in different organisms, only one isoform (*porin*/DVDAC) has been previously reported for *Drosophila melanogaster*. We have examined the physiological properties of three other *Drosophila* proteins (CG17137, CG17139, and CG17140) whose primary sequences have significant homology to DVDAC. A comparison of their hydropathy profiles (β-pattern) with known VDAC sequences indicates the same fundamental folding pattern but with major insertions and deletions. The ability of these proteins to form channels was tested on planar membranes and liposomes. Channel activity was observed with varying degrees of similarity to VDAC. Two of these proteins (CG17137 and CG17140) produced channels with anionic selectivity in the open state. Sometimes channels exhibited closure and voltage gating, but for CG17140 this occurred at much higher voltages than is typical for VDAC. CG17139 was not able to form channels. DVDAC and CG17137 were able to rescue the temperature-sensitive conditional-lethal phenotype of VDAC-deficient yeast, whereas CG17139 and CG17140 demonstrated no complementation. Similar structure and channel formation indicate that VDAC-like proteins are part of the larger VDAC family but the modifications are indicative of specialized functions.

INTRODUCTION

VDAC, also known as mitochondrial porin, is a 30–32 kDa channel-forming protein found in the mitochondrial outer membrane of all eucaryotes (Colombini et al., 1996). It forms an aqueous pore with a diameter of ~3 nm in the open state and 1.8 nm in the closed state. This closed state is still conductive to small ions but effectively impermeant to anionic metabolites (Rostovtseva and Colombini, 1996; Rostovtseva et al., 2002). In the open state VDAC is permeable to nonelectrolytes up to 5000 Da. A model of the secondary structure of VDAC, consisting of one α-helix and 13 β-strands, has been proposed based on a variety of experiments (Song et al., 1998a). These 14 elements form a barrel-like structure that spans the membrane. Other theoretical models have been proposed with a larger number of transmembrane strands (Mannella, 1996). Spectroscopic studies have shown that transmembrane strands are tilted at a 45° angle (Abrecht et al., 2000).

VDAC from disparate eukaryotic species, from different kingdoms, share a form of VDAC with a highly conserved fundamental structure and in vitro electrophysiological properties. The length of the protein ranges between 274 and 295 amino acids. When studied in planar membranes, the channels formed by VDAC demonstrate multiple conductance states with different ionic selectivity: a single open state with high conductance and anionic selectivity, and multiple closed states with low conductance and cationic selectivity. The motion of the voltage-sensitive domain is responsible for channel gating (Song et al., 1998b). In the open state the positively charged voltage sensor is located in the transmembrane region. An increase in voltage causes the movement of the sensor toward the membrane surface resulting in an electrostatic barrier to anionic metabolites and therefore closure of the channel. The numerical values of the functional parameters such as single channel conductance, selectivity, and voltage dependence are very similar for VDAC from different species (Colombini, 1989).

VDAC plays a role in several fundamental cellular processes. By forming the major pathway for metabolite flux across the mitochondrial outer membrane, VDAC is involved in the regulation of metabolite flow across mitochondria and therefore influences mitochondrial function (Vander Heiden et al., 2000, 2001). VDAC may have an important role in the initiation of apoptosis as indicated by its regulation of Ca^{2+}-uptake (Rapizzi et al., 2002) and possible participation in the formation of the permeability transition pore complex (Halestrap et al., 2002). VDAC closure and subsequent interference with ADP/ATP exchange (Vander Heiden et al., 2001) seem to lead to the permeabilization of the outer membrane to proteins resulting in the execution phase of apoptosis. In addition, VDAC has been reported to be a component of the peripheral benzodiazepine receptor complex (McEnery et al., 1992) and may be involved in binding hexokinase and glycerol kinase to mitochondria (Adams et al., 1991). Such a wide variety of functions may require the presence of specialized proteins in the form of isoforms and VDAC-like proteins.

Multiple VDAC isoforms have been identified in numerous diverse species including yeast (Blachly-Dyson et al., 1997), human/mouse (Sampson et al., 1996), and wheat (Elkeles et al., 1995). The electrophysiological characteristics of the prototypic VDAC from different species are highly conserved, yet the biophysical properties of individual

Submitted May 21, 2003, and accepted for publication September 8, 2003.
Address reprint requests to Marco Colombini, E-mail: colombin@umd.edu.

0006-3495/04/01/152/11 $2.00

isoforms from the same species are often quite distinct (Xu et al., 1999). Although the specific functions of individual VDAC isoforms remain to be elucidated, studies with in vivo model systems have given some insights. For example, although VDAC has been implicated in the initiation of apoptosis, one isoform, mammalian VDAC2, interacts with pro-apoptotic BAK to inhibit apoptosis (Cheng et al., 2003). Moreover, when overexpressed, yeast VDAC2 (POR2) was shown to restore normal cell growth in the absence of yeast VDAC1 (POR1) but did not form channels in reconstituted systems (Blachly-Dyson et al., 1997). This implies that a VDAC isoform can be involved in cell survival yet does not necessarily require channel-forming activity. Mice deficient for VDAC isoforms exhibit distinct phenotypes. VDAC1 deficient mice demonstrate altered mitochondrial permeability in skeletal muscle (Anflous et al., 2001), whereas VDAC3 deficient mice are infertile with structural sperm axonemal defects, in addition to respiratory chain abnormalities in muscle (Sampson et al., 2001). Finally, VDAC1, VDAC3, and VDAC1/VDAC3 deficient mice exhibit isoform-specific defects in learning and synaptic plasticity (Weeber et al., 2002).

The recent annotation of the *Drosophila melanogaster* genome (The-FlyBase-Consortium, 2003) revealed three putative VDAC isoforms whose genes are tightly clustered in tandem with the original *Drosophila* VDAC (DVDAC or *porin*) (Oliva et al., 2002). In this article, we describe our studies to characterize the physiological properties of these putative VDAC isoforms.

MATERIALS AND METHODS

Yeast strains and media

M3 (*MATα lys2 his4 trp1 ade2 leu2 ura3*) is the parental wild-type (with respect to *POR1*) strain. M22-2 (*Δpor1*) contains a deletion of *POR1* by insertion of yeast *LEU2* at the *POR1* locus (Blachly-Dyson et al., 1990). The yeast media YPD/SMM (2% dextrose as the carbon source/supplemented with essential nutrients except uracil) and YPG/SMM (3% glycerol as the carbon source/supplemented with essential nutrients except uracil) were prepared as described (Kaiser et al., 1994).

Generation of yeast expression constructs

For *Drosophila* VDAC, oligonucleotide-directed mutagenesis was used to generate a *Nco*I site at the start codon, and a *Nsi*I site in the 3′ UTR. This allowed for the complete open reading frame of the DVDAC cDNA to precisely replace the yeast VDAC1 gene previously subcloned into a single-copy yeast shuttle vector as previously described (Sampson et al., 1997). For *CG17137*, *CG17139*, and *CG17140*, oligonucleotide-directed mutagenesis was used to generate a blunt restriction enzyme site (*Ehe*I for CG17137, *Mly*I for *CG17139*, and *Pme*I for CG17140) at the first codon downstream of the start codon such that, when ligated to the *Nco*I-digested and blunted single-copy yeast shuttle vector, the open reading frame of the yeast VDAC1 is precisely replaced by the corresponding *Drosophila* cDNA. As with DVDAC, either a *Nsi*I (*CG17137* and *CG17139*) or a *Sse 8387*I (*CG17140*) (*Sse 8387*I generates ends compatible with *Nsi*I) site was generated in the 3′ UTR to facilitate cloning. To generate the multiple-copy yeast expression constructs for each *Drosophila* VDAC-like gene, the expression cassette (including the yeast VDAC1 promoter, 5′ and 3′ UTRs) was excised from the corresponding single-copy shuttle construct as a *Bam*H1/*Hind*III fragment and cloned into the 2-μm yeast shuttle vector YEplac195 (Gietz and Sugino, 1988). The sequences of the oligonucleotides are as follows: DVDAC 5′ = GGCAACCATGGCTCCTCCATCATACAG; DVDAC3′ =CCGCGATGCATTCACGACTAGCGGAAAACC; *CG17137* 5′ = GCGAAGGCGCCGCCAAACACCGACATA; *CG17137* 3′ = CCGCGATGCATCGTTAAGTGATTGGCAGT; *CG17139* 5′ = GCGAAGAGTCCCATGAGAGAACGGATA; *CG17139* 3′ = GCGACCTGCAGGCTACATATTGAAGTACCAT; *CG17140* 5′ = GCGAGTTTAAACAACGGCTGCGCAACTT (note that this oligonucleotide also generates a silent G→A mutation in the third position of the first codon downstream of the start codon); *CG17140* 3′ = GCGAATGCATCAACAGTGAAAACCCCAGGAA. The cDNA templates utilized are as follows: *porin* = BDGP (Berkley *Drosophila* Genome Project) Clone ID GM13853 (GenBank AI518978); *CG17137* = BDGP Clone ID AT15574 (GenBank BF500588), *CG17139* = BDGP Clone ID AT07302 (GenBank BF505131), and *CG17140* = AT08366 (GenBank BF506017) (Rubin et al., 2000).

Yeast complementation analysis

Each expression construct was introduced into the *Δpor1 Saccharomyces cerevisiae* strain M22-2 by lithium acetate transformation (Gietz et al., 1992). As controls, wild-type (M3) and *Δpor1* yeast were transformed by the original single- or multiple-copy shuttle vectors. The yeast strains were then grown in 5 ml YPD/SMM liquid cultures at 30°C for 72 h. Each culture was normalized to the M3 cultures based on $OD_{600\ nm}$ and spotted onto 2 YPG/SMM plates as six-serial fivefold dilutions. The plates were incubated at 30°C or 37°C respectively for 6 days.

Preparation of yeast cells

To facilitate cell growth and harvesting, stock cultures were prepared. A colony of yeast cells, containing one of the VDAC-like genes, was inoculated into 50 ml medium consisting of 95 mg yeast nitrogen base (No. 0335-15-9, DIFCO LABORATORIES, Detroit, MI), 250 mg ammonium sulfate, 1 g dextrose, and 38.5 mg CSM-URA (No. 4511-222, Complete Supplement Mixture minus Uracil; Q-BIOgene, Carlsbad, CA). When the cells reached an OD of between 0.6 and 0.8 (at 600 nm) they were stored at 4°C for later use. For mitochondrial isolation, 9 ml yeast stock solution was inoculated into each of two flasks containing 1 L of the same medium and grown with shaking at 30°C. An OD between 0.7 and 0.8 was reached at 41 h after inoculation. Typically, 5–8 g of cells was obtained. A total of 5 g of cells was used for the isolation of mitochondria.

Isolation of VDAC-like proteins

Mitochondria were isolated from *S. cerevisiae* essentially as published by Daum et al. (1982) but modified as previously described (Lee et al., 1998). The final mitochondrial suspension was hypotonically shocked in 1 mM KCl, 1 mM HEPES, pH 7.5 to break the mitochondrial membranes and release soluble proteins. The membranes were sedimented at 24,000 *g* for 20 min.

VDAC-like proteins were isolated from mitochondrial membranes and purified according to standard methods (Mannella, 1982; Freitag et al., 1983). The last step was a 1:1 hydroxyapatite/celite column that, at low ionic strength, binds most proteins but allows VDAC to flow through. This also is a property of VDAC-like proteins.

Channel conductance measurements

Planar membranes were formed from monolayers made from a solution containing 0.5% diphytanoylphosphatidylcholine, 0.5% asolectin-soybean phospholipid (both were from Avanti Polar Lipids, Alabaster, AL), and 0.1% cholesterol (Sigma, St. Louis, MO) in hexane. The two monolayers formed

a bilayer membrane across a 70–90-μm diameter aperture in a 15-μm thick Teflon partition that separated two chambers (modified Montal and Mueller technique; Montal and Mueller, 1972). The total capacitance was 70–80 pF and the film capacitance was 30–35 pF. Aqueous solutions of 1.0 M or 0.10 M NaCl and 1 mM $MgCl_2$ (in some experiments additional 1 mM $CaCl_2$ was present) were buffered by 5 mM HEPES at pH 7.0. All measurements were made at room temperature.

Channel insertion(s) was achieved by adding 0.2–2.0 μl 1% Triton X100 solution of purified VDAC-like protein to the 2.5 ml aqueous phase in the *cis* compartment while stirring.

The membrane potential was maintained using Ag/AgCl electrodes with 3.0 M KCl, 15% agarose bridges assembled within standard 200-μl pipette tips (Bezrukov and Vodyanoy, 1993). Potential is defined as positive when it is greater at the side of protein addition (*cis*). The current was amplified by an Axopatch 200B amplifier (Axon Instruments, Foster City, CA) in the voltage clamp mode.

Reversal potential measurements

The reversal or zero-current potential was measured to assess the selectivity in single or multichannel membranes. A positive reversal potential on the high salt side slows down the flux of anions down their gradient and increases the flux of cations. If a positive potential brings the current to zero then the channel must pass anions more readily than cations (i.e., has anionic selectivity). A negative potential would indicate cation selectivity. We used a 10-fold gradient of NaCl, 1.0 M *cis* and 0.10 M *trans*, plus Mg^{2+} and HEPES as above. An aliquot of solution containing VDAC-like protein was added to the side with higher concentration. As the channels can exist in different conformations each with different selectivity, triangular voltage waves were applied and the reversal potential of each state obtained by extrapolating the current record to zero current (see Fig. 6).

Liposome permeability measurements

The liposomes were made as follows (Colombini, 1980): 22.5 mg egg phosphatidyl-choline (Sigma) and 2.0 mg egg phosphatidylserine (Avanti Polar Lipids), both dissolved in chloroform, were mixed together and dried down under N_2. A quantity of 1 ml 1 mM KCl, 1 mM HEPES, pH 7.0 solution was added to the dry lipids and the material was sonicated (at 0–5°C). A quantity of 1 ml mitochondrial membranes suspended in 1 mM KCl, 1 mM HEPES, pH 7.0 containing 1.2 mg protein was mixed into the lipid solution prepared above. The mixture was sonicated again and lyophilized overnight. Liposomes were produced by dispersing the dry material in 1 ml 20 mM KCl, 1 mM EDTA, pH 7.0.

A total of 50 μl of this liposome suspension were added to 0.8 ml 20 mM KCl, 1 mM EDTA, pH 7.0, and the absorbance at 400 nm was monitored. Nonelectrolytes of different molecular weight were dissolved in the same solution and added to the liposomes when the liposomes had stabilized (no change in absorbance with time). One might expect that upon shrinkage the KCl concentration in the liposomes would increase resulting in extended shrinkage as the KCl redistributes with time. In fact, in these liposomes K^+ and Cl^- flux is so fast that these redistribute almost as rapidly as water. Indeed, if hypertonic KCl is used to attempt to shrink the liposomes, there is almost no shrinkage.

SDS-page electrophoresis

To determine whether we have VDAC-like proteins in the final fraction of the purification procedure, we used standard SDS-page electrophoresis procedure (Laemmli, 1970). Equal aliquots of solutions containing VDAC or VDAC-like proteins were mixed with concentrated sample buffer. Samples were separated on a 12% acrylamide gel supplemented with 4 M urea and the bands stained with GelCode Blue stain (Pierce, Rockford, IL).

RESULTS

In addition to VDAC, *D. melanogaster* expresses three proteins whose primary sequences resemble that of VDAC, the VDAC-like proteins. The question to be addressed is how similar are these proteins to VDAC in terms of structure and function.

DVDAC and CG17137 rescue the conditional lethal phenotype of yeast cells deficient for VDAC1

Our initial approach for analyzing the function of the VDAC-like genes in *D. melanogaster* was to individually express them in a yeast strain that is deficient for the endogenous VDAC1 gene (*Δpor1*). The *Δpor1* strain is characterized by a temperature-dependent growth-restrictive phenotype when cultured on a nonfermentable carbon source such as glycerol: cells are able to grow at 30°C, but not 37°C (Blachly-Dyson et al., 1990). It has been previously demonstrated that mammalian VDACs expressed in the *Δpor1* background rescue this conditional phenotype, allowing growth on glycerol at 37°C (Blachly-Dyson et al., 1993; Sampson et al., 1997). Ryerse et al. previously reported that DVDAC failed to complement *Δpor1* yeast (Ryerse et al., 1997). However, we observed that DVDAC does indeed complement *POR1* function in *Δpor1* yeast when expressed from the *POR1* promoter on either a single-copy (CEN) or a multiple-copy (2 μm) yeast shuttle vector (Fig. 1). Additionally, we observed that *CG17137* rescued the *Δpor1* conditionally growth-restrictive phenotype when expressed from the single-copy vector. *CG17139* and *CG17140* both failed to

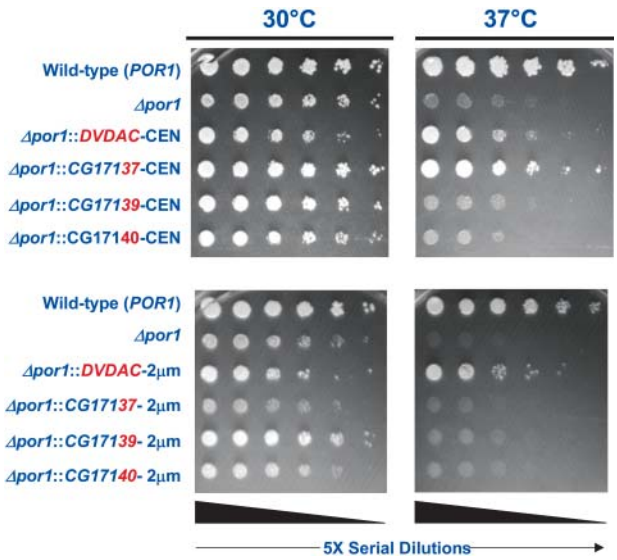

FIGURE 1 Complementation analysis of DVDAC and VDAC-like genes in yeast. Wild-type (*POR1*), *Δpor1*, or *Δpor1* yeast transformed with the indicated expression constructs plated on 3% glycerol and grown at the indicated temperatures are shown. In each panel, each row represents six serial fivefold dilutions of each strain as indicated.

complement *Δpor1* yeast whether expressed from single-copy or multiple-copy vector (Fig. 1).

Sequence analysis indicates a VDAC-like secondary structure

The alignment of the amino acid sequences for *D. melanogaster* VDAC and CG17137 shows extensive sequence identity between these two polypeptides (Fig. 2). CG17139 and CG17140, although far more similar to each other (including the N-terminal extension) also exhibit significant sequence similarity with VDAC, especially near the N- and C-termini. In agreement with Oliva et al. (2002), pairwise alignment of these polypeptides reveal 42% identity and 65% similarity with DVDAC for CG17137, 23% identity and 42% similarity for CG17139, and 26% identity and 44% similarity for CG17140. These values are much lower than those previously reported for VDAC isoforms from the same species (yeast, mouse, and wheat); however, they are in the same range as the values obtained from comparisons of VDAC sequences from diverse organisms. For example, human and yeast VDAC have less than 30% sequence identity (Blachly-Dyson and Forte, 2001). In fact, pairwise alignment of these *Drosophila* polypeptides with mouse VDAC1 reveal 58% identity and 75% similarity for DVDAC, 34% identity and 56% similarity for CG17137, 24% identity and 39% similarity for CG17139, and 21% identity and 38% similarity for CG17140. However, even sequences with low primary sequence identity form channels with very similar conductance and ion selectivity. This means that, despite divergence in the primary sequence, these proteins should have a very similar secondary structure.

Our analysis of CG17137, CG17139, and CG17140 for secondary structure homology with VDAC is based on looking for patterns of alternating hydrophobic and hydrophilic residues that are required to form transmembrane β-strands lining the wall of a β-barrel channel. For this purpose we generated the β-pattern profile as described by Blachly-Dyson et al. (1989). A β-pattern parameter (β) was calculated for each group of 10 adjacent amino acids by combining the hydropathy value (Kyte and Doolittle, 1982) of each as follows:

$$\beta = \left| \sum_{i=1}^{10} (-1)^{i+1} \nu(i) \right|, \qquad (1)$$

where $\nu(i)$ is the hydropathy value of the ith amino acid. This yields large numbers for a fragment that has alternating polar-nonpolar pattern. The β-pattern parameters were plotted against the number of the first amino acid in the group. Analysis of *Drosophila* peptide sequences reveals peaks for the location of putative transmembrane strands

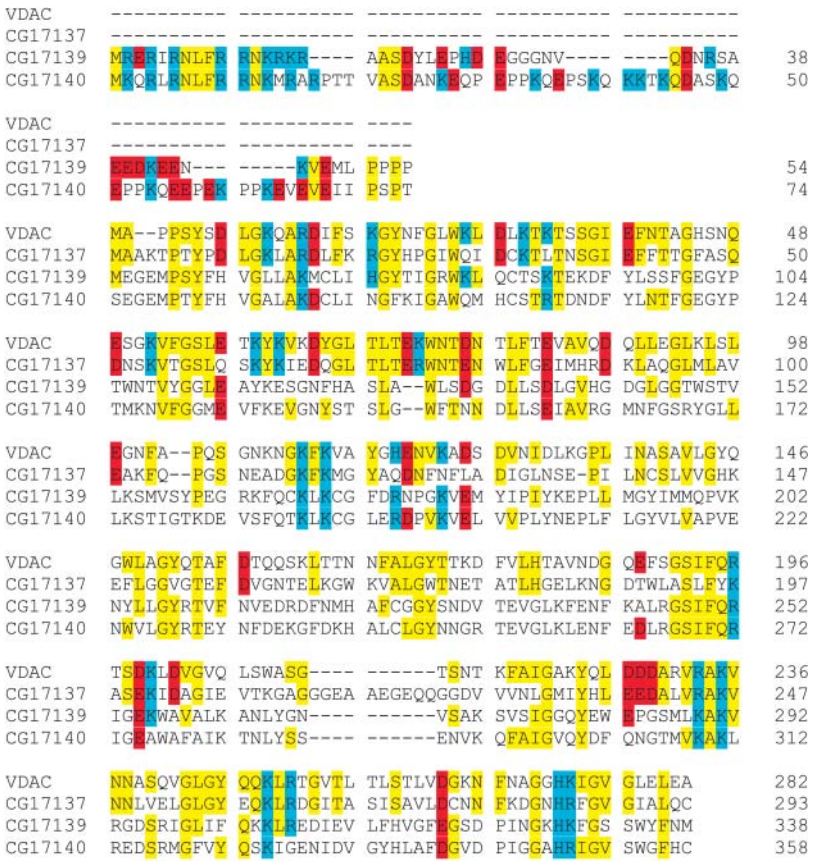

FIGURE 2 The amino acid sequence of the *D. melanogaster* VDAC was aligned with VDAC-like sequences CG17137, CG17139, and CG17140. Colored boxes show matches between VDAC and any of the other sequences: yellow for uncharged amino acids, red for negative charged amino acids, and blue for positive charged amino acids. For the case of N-terminus extensions of CG17139 (1–54 amino acids) and CG17140 (1–74 amino acids) colored boxes indicate matches between the two sequences as well as all charged amino acid residues.

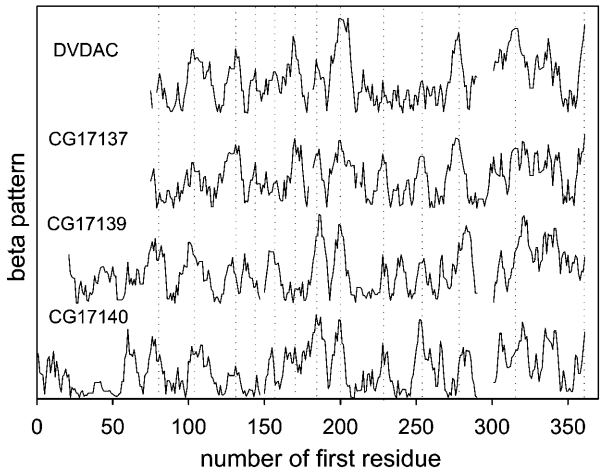

FIGURE 3 A comparison of the β-patterns (see text) of *D. melanogaster* VDAC, CG17137, CG17139, and CG17140. The dotted lines show similarity in location of the peaks. The gaps were generated based on the results of the primary structure alignment.

(Fig. 3). These peaks correlate rather well with each other. The overall correlation coefficients are shown in Table 1. These are all highly statistically significant (>99%), but clearly there is stronger similarity between DVDAC and CG17137, and between CG17139 and CG17140. These results indicate that all compared sequences might share a similar secondary structure and a similar number of putative transmembrane strands.

To test the possibility that the three VDAC-like sequences are in fact channel-forming isoforms of *D. melanogaster* VDAC, the gene products for *CG17137*, *CG17139*, and *CG17140* were purified from mitochondrial outer membranes isolated from *Δpor1* yeast expressing these genes and utilized for electrophysiological studies in reconstituted systems in vitro.

TABLE 1 Correlation coefficients of β-patterns

	DVDAC	CG17137	CG17139
CG17137	0.70		
CG17139	0.39	0.34	
CG17140	0.46	0.39	0.63

CG17137 forms typical VDAC channels

We examined the ability of CG17137 to increase the conductance of planar phospholipid membranes formed under standard conditions (see Materials and Methods). The detergent-solubilized protein was added to the aqueous phase on one side of the membrane and, after some time, conductance increments were observed. Fig. 4 *A* shows the insertion of a 0.31-nS conductance. This conductance responded to the application of elevated voltages by closing transitions reminiscent of VDAC. However, this was not always the case. In fact, results obtained with this protein were rather variable. CG17137 forms discrete conducting events but we were not able to identify, with confidence, a conductance characteristic of a single channel. The data suggest conducting pathways in the range of 0.5–8 nS in the presence of 1.0 M NaCl and 0.13–0.46 nS at the presence of 0.10 M NaCl. Based on the known properties of VDAC, one might propose that this range corresponds to a variety of different conductance states of a channel. The voltage dependent gating illustrated in Fig. 4 *B* and upon application of a triangular voltage wave (Fig. 5) is reminiscent of classical VDAC behavior. However, attempts at further confirmation by looking at selectivity changes associated with gating revealed a complex pattern. We assessed the selectivity by making measurements in the presence of a salt concentration gradient and extrapolating linear segments to determine the zero-current potential. As expected, conductance changes were associated with changes in the selectivity

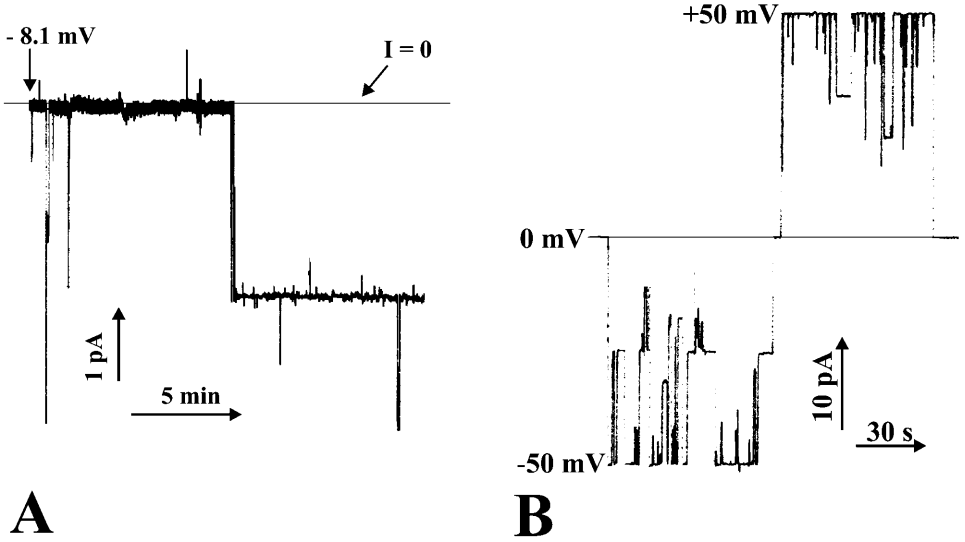

FIGURE 4 Changes in ionic current through a planar membrane in the presence of CG17137. Both compartments contained 0.10 M NaCl. (*A*) Insertion of the channel. (*B*) Gating of the channel at high voltages.

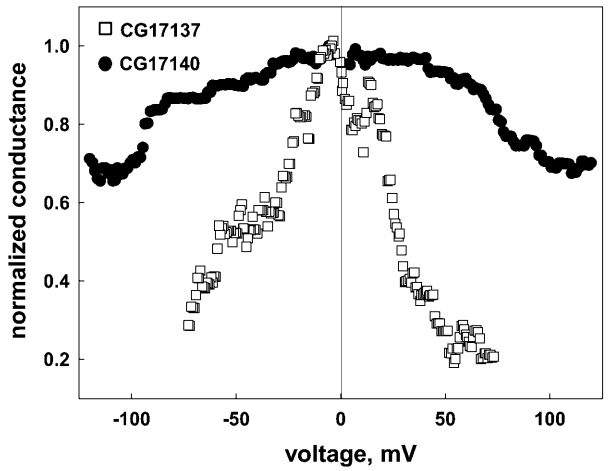

FIGURE 5 Voltage dependence of the conductance of the channels formed by CG17137 and CG 17140. The voltage was applied in the form of triangular waves (3 mHz, ±73 mV for CG17137 and ±120 mV for CG17140). The membranes contained 2–4 channels.

of the channel(s) (Fig. 6 *A*). Negative voltages correspond to a conductance with cationic selectivity and positive voltages with anionic selectivity. A single VDAC channel demonstrates anionic selectivity in the open state and cationic selectivity in the lower conducting closed states. In the case of conductance formed by CG17137 we observed that sometimes the closure of the channel(s) did result in a change toward a preference for cations but at other times the opposite was true. This inconsistency might be explained by a mixture of channel gating and channel insertion or disappearance but variability in the observed conductances also made it difficult to distinguish between these possibilities.

CG17139 does not demonstrate channel formation

In experiments with planar membranes we were not able to get an increase in membrane conductance after addition of CG17139. Our observations were conducted under varied conditions: different salt concentrations (0.1 M or 1 M), salts of sodium or potassium, pH 6.0–8.0, presence of different divalent ions (Ca^{2+} or Mg^{2+}). In all cases we observed a lack of channel formation.

CG17140 also forms channels

Fig. 7 *A* shows discrete increases in the conductance of planar membranes after addition of detergent-solubilized CG17140. The observed single channel conductance was 1.38 ± 0.12 nS (mean ± SD) in 1.0 M NaCl. The channels gate (Fig. 7 *B*) but only at very high applied voltages (110 mV and higher; Fig. 7 *B*). Closure of a normal VDAC channel is observed at 30 mV and higher. Fig. 5 shows voltage-dependent closure at both positive and negative voltages but closure is incomplete in the voltage range tested. In the presence of a 10-fold salt

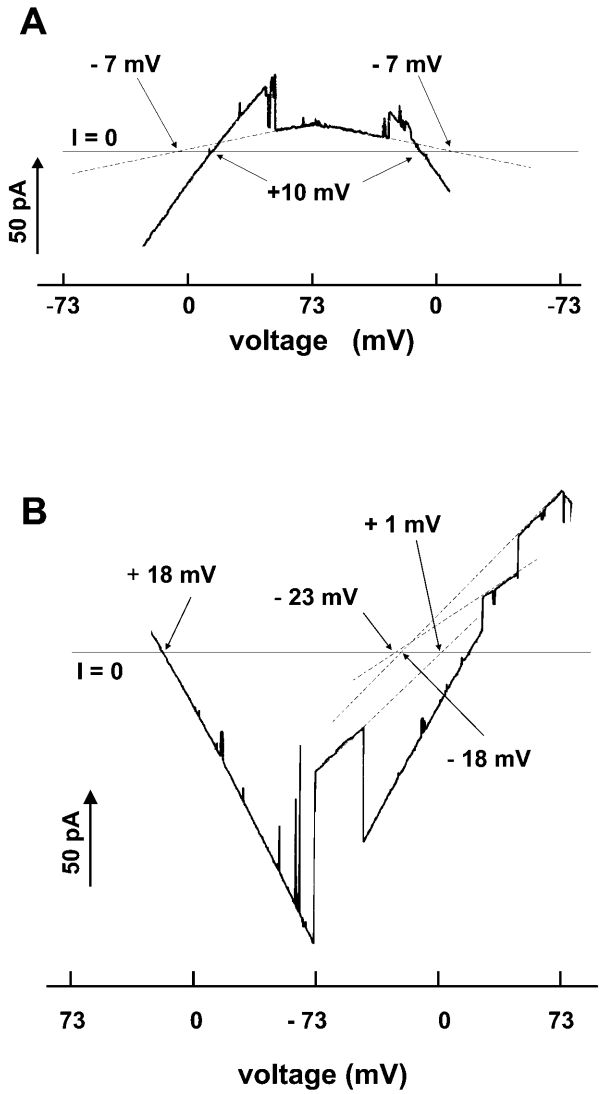

FIGURE 6 Selectivity of the channel(s) formed by CG17137 (*A*) and CG17140 (*B*) in the presence of a salt gradient. In the case with CG17140 both compartments also contained 1 mM $CaCl_2$. The indicated voltage refers to the *cis* side. The voltage was applied in the form of slow triangular waves (3 mHz, ±73 mV). The dotted lines are extrapolations used to determine the reversal potential of each selected conductance level. The numbers associated with the zero-current intercepts show the value of the reversal potential.

gradient, CG17140 demonstrated a conductance of 0.61 ± 0.02 nS and a reversal potential of + 22.6 ± 2.4 mV, corresponding to anionic selectivity. Closure of these channels resulted in a switch to cationic selectivity with varying values of the reversal potential (Fig. 6 *B*). This is in agreement with typical VDAC behavior.

CG17137, CG17139, and CG17140 cause differential permeabilization of liposomes

The use of planar membranes to assess the ability of the VDAC-like proteins to form channels has the drawback that

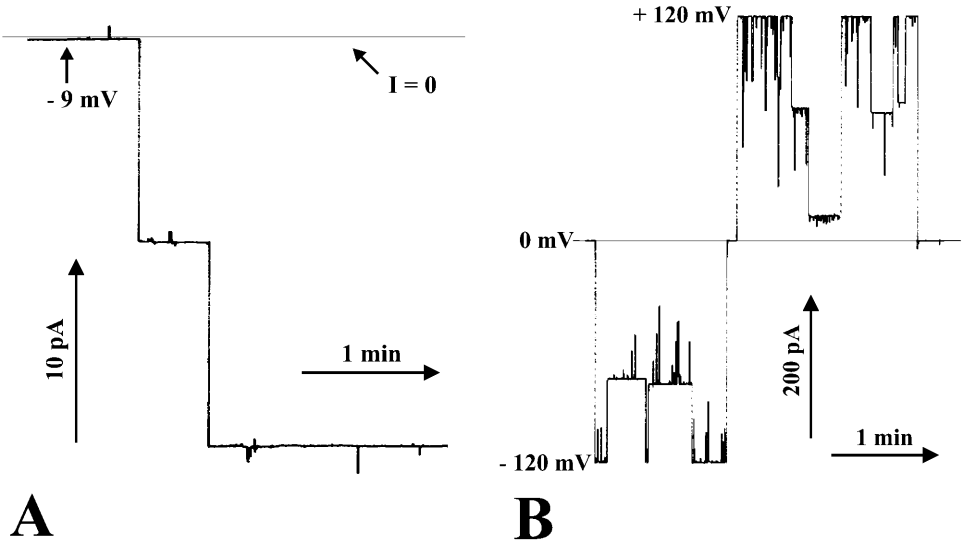

FIGURE 7 Changes in ionic current through a planar membrane in the presence of CG17140. Both compartments contained 1.0 M NaCl. (*A*) Insertion of two channels. (*B*) Gating of the channels at high voltage.

one is selecting for proteins that insert into the membranes. It is possible that a minor constituent might be responsible for the observed activity. The use of liposomes allows one to assess the ability of the population to permeabilize membranes. It also eliminates the need for the protein to insert into the membrane from an aqueous environment.

We incorporated CG17137, CG17139, and CG17140 into liposomes and measured the permeability of the liposomes, using hyperosmotic solutions of nonelectrolytes of different sizes. Mixing of liposomes with these solutions induces liposome shrinkage due to the fact that water moves out of the liposomes faster than the solute can move in. In the case of a permeable solute, reswelling follows the shrinkage of the liposomes. The shrinkage-reswelling process was observed by measuring changes in light scattering at 400 nm over time. A decrease of the liposome size causes an increase in apparent absorbance and a decrease of absorbance indicates reswelling of the liposomes. The rate of reswelling reflects the permeability of the liposome membrane. If the solute is impermeable it will demonstrate a lack of reswelling. Using this method we can also estimate the molecular weight cutoff of the permeability pathway.

Fig. 8 shows the absorbance traces for liposomes containing the VDAC-like proteins. The initial absorbance is due to rapid shrinkage resulting from the hypertonic stress of the indicated nonelectrolyte. This was followed by various rates of absorbance reduction due to permeation of nonelectrolyte into the liposomes. In CG17137-containing liposomes (*top* panel), reswelling occurred with all except the highest molecular weight of nonelectrolyte (PEG 6800). This molecular weight cutoff is the same as that reported for VDAC (Colombini, 1980). For CG17140-containing liposomes, the molecular weight cutoff was somewhat lower. The results show no significant reswelling in the presence of γ-cyclodextrin (1300 Da). The liposomes containing CG 17139 did not show significant reswelling with PEG 1500 (the slight decline was not different from control). The CG17139-containing liposomes did show permeability to PEG 1000, but this was also observed when liposomes were formed using mitochondrial membranes isolated from yeast lacking VDAC1 (Fig. 8, panel *E*, in Xu et al., 1999). Thus there is no detectable permeability increase by the presence of CG17139.

DISCUSSION

The study of the physiological properties of VDAC-like proteins in reconstituted systems (planar membranes and liposomes) is a step in understanding their specialized cellular functions. We used both theoretical and experimental methods for characterization of these proteins. Insights gained from previous publications have allowed us to predict and explain the behavior of the recently discovered VDAC-like proteins. Their similar properties to those of classical VDAC may indicate that some of these proteins are actually VDAC isoforms.

The VDAC-like proteins from *D. melanogaster* were tested for the major VDAC property, the ability to form voltage-dependent channels with characteristic channel size and ion selectivity. CG17137 and CG17140 clearly demonstrate channel-forming activity in both planar phospholipid membranes and in liposomes, CG17139 does not. The voltage dependence and selectivity are also reminiscent of classical VDAC behavior.

Insight into the physiological properties of these proteins was obtained by determining their ability to rescue the conditional lethal phenotype of yeast deficient for VDAC1 (POR1). We demonstrated that DVDAC and *CG17137* can rescue VDAC-deficient yeast, whereas *CG17139* and *CG17140* cannot. It is unclear why Ryerse et al. could not demonstrate complementation with DVDAC (Ryerse et al., 1997). This complementation pattern roughly correlates to

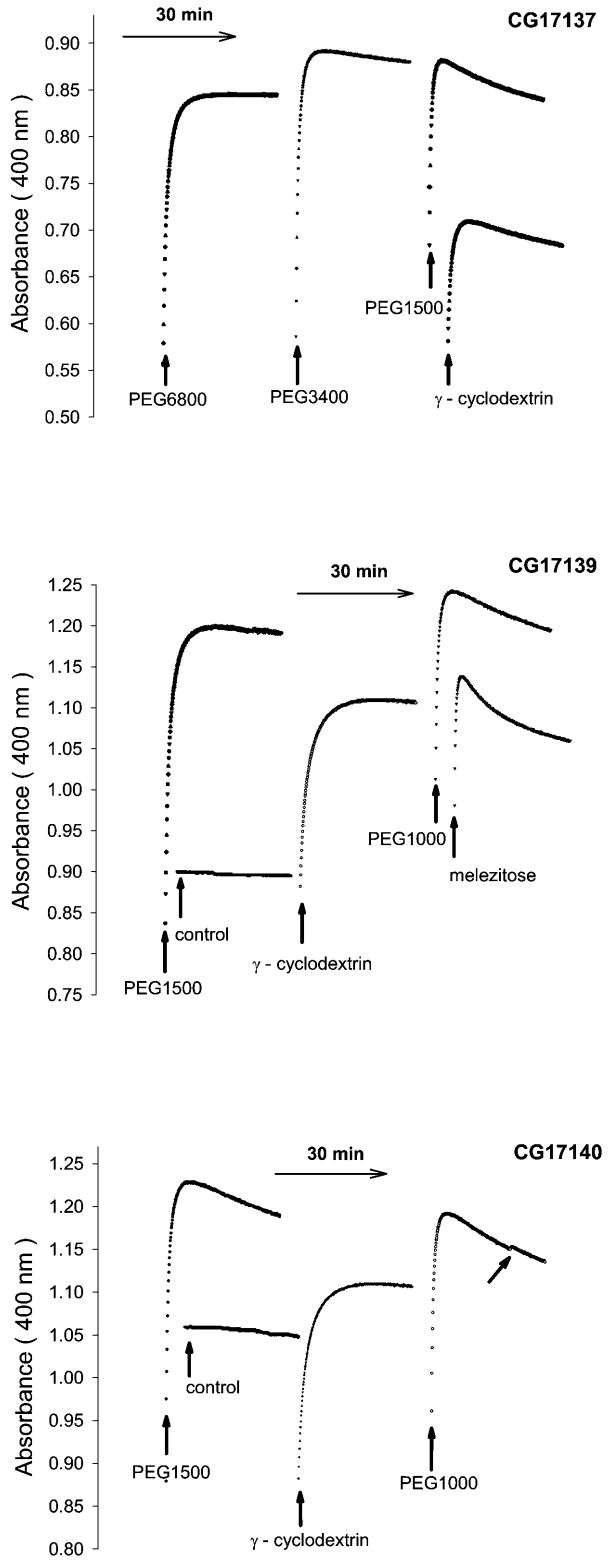

FIGURE 8 The responses of liposomes containing one of the proteins CG17137, CG17139, and CG17140 to osmotic pressure changes caused by nonelectrolytes. The liposomes were made as described in Material and Methods. The absorbance at 400 nm was recorded. When the liposomes had stabilized (no significant change in absorbance, ~1 h after dilution) 67 μl 50 mM PEG6800, 67 μl 100 mM PEG3400, 67 μl 100 mM PEG1500, 220 μl 20 mM γ-cyclodextrin, 67 μl 225 mM PEG1000, or 67 μl 278 mM melezitose was added and quickly mixed at the point shown by the vertical arrows. All tracings in each panel were performed on the same set of liposomes so these can be readily compared. The tilted arrow indicates the brief mixing of the sample during recording showing no significant sedimentation of the liposomes.

the observed biophysical characteristics of these proteins, with DVDAC demonstrating classical VDAC properties as previously reported (De Pinto et al., 1989). We have demonstrated that CG17137 also exhibits properties similar to those of classical VDAC in planar membranes and liposomes in terms of voltage gating and liposomal permeability. On the other hand, channels formed by CG17140 demonstrate conductance that is ~40% of DVDAC or other classical VDACs and a smaller aqueous pore as indicated by the impermeability to γ-cyclodextrin (MW 1300), whereas CG17139 fails to form channels in either planar membranes or liposomes. The reduced size of the aqueous pore formed by CG17140 may restrict the flow of some critical metabolite resulting in failure of cells to grow at 37°C. In any case, of the three VDAC-like proteins, only CG17137 has properties similar enough to VDAC to functionally substitute for VDAC and thus could be an isoform of *Drosophila* VDAC.

The high degree of similarity between the β-pattern of *D. melanogaster* VDAC and CG17137 indicates that they might share similar folding patterns. To view our results in the context of predicted secondary structures, we generated the folding patterns (Fig. 9) for all studied proteins by analogy with *Neurospora crassa* VDAC (Song et al., 1998a). The choice of candidate transmembrane β-strands was based on the following criteria: 1), A candidate strand should have a good alternating hydrophilic and hydrophobic pattern; 2), Chain-distorting prolines should not be located in the middle of the transmembrane strand but rather at the ends of the strands; 3), There should be no adjacent charged amino acids except at the ends; 4), The strand should have good sequence homology to the corresponding transmembrane β-strand for *N. crassa* VDAC.

When comparing the secondary structure of CG17137 to the *Drosophila* VDAC folding pattern, the major difference is a 10 amino acid insertion in the long loop region on the cytosolic face of CG17137 (Fig. 9 *A*). This insertion adds three negative charges to the long loop region, which is already rich in charged residues. In fungi, this region between position 184 and 228 is not involved in either voltage gating or selectivity (Thomas et al., 1993; Blachly-Dyson et al., 1994) and may serve as a binding site for a cytosolic factor. Indeed, the major difference between human VDAC1 (HVDAC1) and human VDAC2 (HVDAC2) is a change from KK to ED at position 199-200 on HVDAC1 and perhaps this explains why HVDAC1 binds hexokinase and HVDAC2 does not (Blachly-Dyson et al., 1993). This change may be sufficient to favor interaction with a specific cytosolic factor. There are other differences between

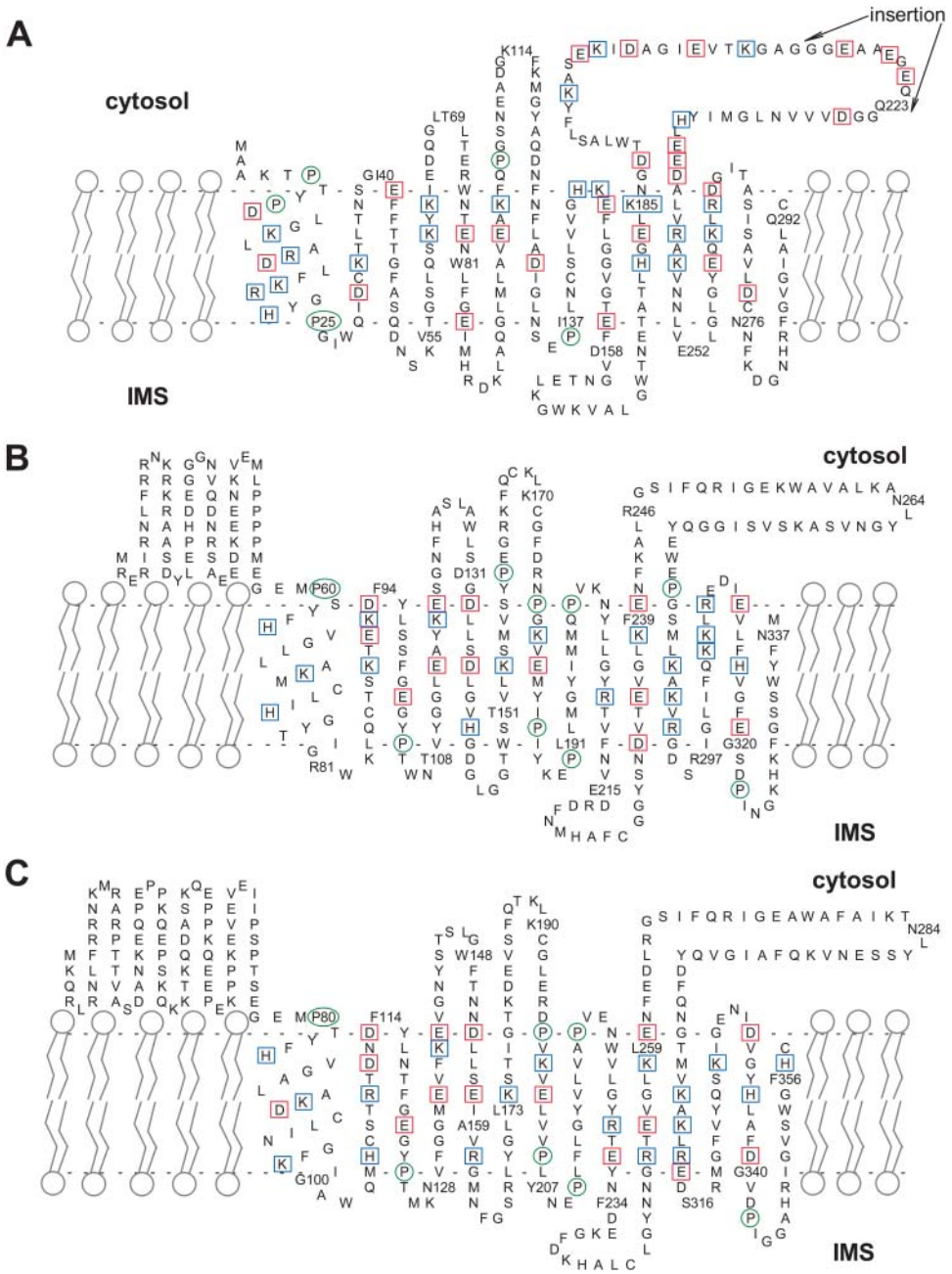

FIGURE 9 The folding patterns for CG17137 (*A*), CG17139 (*B*), and CG17140 (*C*). The long loop region for CG17137 and the membrane regions have been highlighted: green circles, prolines; blue boxes, positively charged amino acid residues; red boxes, negatively charged amino acid residues. IMS, intermembrane space.

CG17137 and *Drosophila* VDAC and some of these are likely responsible for the differences in the properties of the single channels that were observed. Additionally, the variability of the observed channels formed by CG17137 may indicate the absence of a factor or factors that act to limit the number of structural states. The limiting of variable behavior by VDAC when interacting with controlling factors has been observed on a number of occasions (for example, Holden and Colombini, 1988).

The sequences of CG17139 and CG17140 differ from both CG17137 and *D. melanogaster* VDAC in having long, highly charged, N-terminus extensions (Fig. 9). The role of this feature is unclear. The mouse VDAC2 isoform has such an extension, albeit considerably shorter, but forms channels with canonical VDAC properties. Perhaps, the highly charged N-terminus extensions could serve as a binding site for agents stimulating unknown activities of VDAC-like proteins.

Protein CG17139 differs from the other VDAC-like proteins in its inability to form channels either in planar membranes or in liposomes. Lack of channel formation in planar membranes could be attributed to inability to insert from the aqueous phase. However, the liposomes were formed from a protein-lipid mixture, and thus the protein

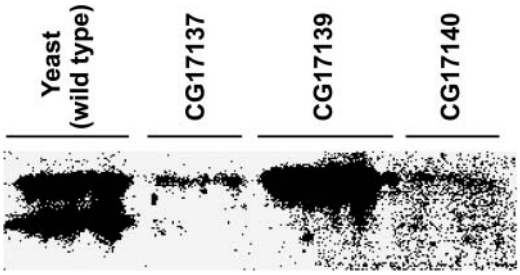

FIGURE 10 SDS-PAGE electrophoresis image of yeast VDAC and VDAC-like proteins. The proteins were purified from mitochondrial membranes and run on 12% acrylamide gel. The upper band shown for each sample ran at ~36 kDa.

must have been present in the liposomal membrane. To test the possibility that insufficient protein was present SDS-PAGE of the purified VDAC fractions from the expression yeast strains was performed (Fig. 10). Clearly the yield of CG17139 purified from the same amount of yeast cells was even larger than that obtained for CG17137 or CG17140.

The folding pattern generated for CG17139 (Fig. 9 *B*) may explain its inability to form channels. Colored squares indicate the presence of consecutive charged residues in the 1st and 11th β-transmembrane strands, which conflicts with the restrictions mentioned above and should inhibit formation of the channel. CG17140 does not have this feature (Fig. 9 *C*), and its folding pattern is consistent with the fact that channels were observed.

In conclusion, our results indicate that despite the low degree of primary sequence identity with *Drosophila* VDAC, VDAC-like proteins have retained aspects of VDAC structure and function. The differential ability to complement VDAC-deficient yeast, and varied in vitro biophysical properties suggest that the members of this gene family in *Drosophila* play distinct physiological roles that need to be elucidated with future in vivo studies.

This work was supported in part by National Institutes of Health NRSA 1F32GM065041-01 (B.H.G.), Baylor Child Health Research Center Scholarship (B.H.G.), National Institutes of Health RO1 N5042319 (W.J.C.), and National Institutes of Health R01 NS42319 (M.C.).

REFERENCES

Abrecht, H., E. Goormaghtigh, J. M. Ruysschaert, and F. Homble. 2000. Structure and orientation of two voltage-dependent anion-selective channel isoforms. An attenuated total reflection fourier-transform infrared spectroscopy study. *J. Biol. Chem.* 275:40992–40999.

Adams, V., L. Griffin, J. Towbin, B. Gelb, K. Worley, and E. R. McCabe. 1991. Porin interaction with hexokinase and glycerol kinase: metabolic microcompartmentation at the outer mitochondrial membrane. *Biochem. Med. Metab. Biol.* 45:271–291.

Anflous, K., D. D. Armstrong, and W. J. Craigen. 2001. Altered mitochondrial sensitivity for ADP and maintenance of creatine-stimulated respiration in oxidative striated muscles from VDAC1-deficient mice. *J. Biol. Chem.* 276:1954–1960.

Bezrukov, S. M., and I. Vodyanoy. 1993. Probing alamethicin channels with water-soluble polymers. Effect on conductance of channel states. *Biophys. J.* 64:16–25.

Blachly-Dyson, E., A. Baldini, M. Litt, E. R. McCabe, and M. Forte. 1994. Human genes encoding the voltage-dependent anion channel (VDAC) of the outer mitochondrial membrane: mapping and identification of two new isoforms. *Genomics.* 20:62–67.

Blachly-Dyson, E., and M. Forte. 2001. VDAC channels. *IUBMB Life.* 52:113–118.

Blachly-Dyson, E., S. Z. Peng, M. Colombini, and M. Forte. 1989. Probing the structure of the mitochondrial channel, VDAC, by site-directed mutagenesis: a progress report. *J. Bioenerg. Biomembr.* 21:471–483.

Blachly-Dyson, E., S. Peng, M. Colombini, and M. Forte. 1990. Selectivity changes in site-directed mutants of the VDAC ion channel: structural implications. *Science.* 247:1233–1236.

Blachly-Dyson, E., J. Song, W. J. Wolfgang, M. Colombini, and M. Forte. 1997. Multicopy suppressors of phenotypes resulting from the absence of yeast VDAC encode a VDAC-like protein. *Mol. Cell. Biol.* 17:5727–5738.

Blachly-Dyson, E., E. B. Zambronicz, W. H. Yu, V. Adams, E. R. McCabe, J. Adelman, M. Colombini, and M. Forte. 1993. Cloning and functional expression in yeast of two human isoforms of the outer mitochondrial membrane channel, the voltage-dependent anion channel. *J. Biol. Chem.* 268:1835–1841.

Cheng, E. H.-Y., T. Sheiko, J. K. Fisher, W. J. Craigen, and S. J. Korsmeyer. 2003. VDAC2 inhibits BAK activation and mitochondrial apoptosis. *Science.* 301:513–517.

Colombini, M. 1980. Structure and mode of action of a voltage dependent anion-selective channel (VDAC) located in the outer mitochondrial membrane. *Ann. N. Y. Acad. Sci.* 341:552–563.

Colombini, M. 1989. Voltage gating in the mitochondrial channel, VDAC. *J. Membr. Biol.* 111:103–111.

Colombini, M., E. Blachly-Dyson, and M. Forte. 1996. VDAC, a channel in the outer mitochondrial membrane. *In* Ion Channels, Vol. 4. T. Narahashi, editor. Plenum Press, New York. 169–202.

Daum, G., P. C. Bohni, and G. Schatz. 1982. Import of proteins into mitochondria. Cytochrome b2 and cytochrome c peroxidase are located in the intermembrane space of yeast mitochondria. *J. Biol. Chem.* 257:13028–13033.

De Pinto, V., R. Benz, C. Caggese, and F. Palmieri. 1989. Characterization of the mitochondrial porin from Drosophila melanogaster. *Biochim. Biophys. Acta.* 987:1–7.

Elkeles, A., K. M. Devos, D. Graur, M. Zizi, and A. Breiman. 1995. Multiple cDNAs of wheat voltage-dependent anion channels (VDAC): isolation, differential expression, mapping and evolution. *Plant Mol. Biol.* 29:109–124.

Freitag, H., R. Benz, and W. Neupert. 1983. Isolation and properties of the porin of the outer mitochondrial membrane from Neurospora crassa. *Methods Enzymol.* 97:286–294.

Gietz, D., A. St Jean, R. A. Woods, and R. H. Schiestl. 1992. Improved method for high efficiency transformation of intact yeast cells. *Nucleic Acids Res.* 20:1425.

Gietz, R. D., and A. Sugino. 1988. New yeast-Escherichia coli shuttle vectors constructed with in vitro mutagenized yeast genes lacking six-base pair restriction sites. *Gene.* 74:527–534.

Halestrap, A. P., G. P. McStay, and S. J. Clarke. 2002. The permeability transition pore complex: another view. *Biochimie.* 84:153–166.

Holden, M. J., and M. Colombini. 1988. The mitochondrial outer membrane channel, VDAC, is modulated by a soluble protein. *FEBS Lett.* 241:105–109.

Kaiser, C., S. Michaelis, and A. Mitchell. 1994. Methods in Yeast Genetics: A Cold Spring Harbor Laboratory Course Manual. Cold Spring Harbor Laboratory Press, Cold Spring Harbor, NY.

Kyte, J., and R. F. Doolittle. 1982. A simple method for displaying the hydropathic character of a protein. *J. Mol. Biol.* 157:105–132.

Laemmli, U. K. 1970. Cleavage of structural proteins during the assembly of the head of bacteriophage T_4. *Nature (Lond.).* 227:680–685.

Lee, A. C., X. Xu, E. Blachly-Dyson, M. Forte, and M. Colombini. 1998. The role of yeast VDAC genes on the permeability of the mitochondrial outer membrane. *J. Membr. Biol.* 161:173–181.

Mannella, C. A. 1982. Structure of the outer mitochondrial membrane: ordered arrays of porelike subunits in outer-membrane fractions from Neurospora crassa mitochondria. *J. Cell Biol.* 94:680–687.

Mannella, C. A. 1996. Mitochondrial channels revisited. *J. Bioenerg. Biomembr.* 28:89–91.

McEnery, M. W., A. M. Snowman, R. R. Trifiletti, and S. H. Snyder. 1992. Isolation of the mitochondrial benzodiazepine receptor: association with the voltage-dependent anion channel and the adenine nucleotide carrier. *Proc. Natl. Acad. Sci. USA.* 89:3170–3174.

Montal, M., and P. Mueller. 1972. Formation of bimolecular membranes from lipid monolayers and a study of their electrical properties. *Proc. Natl. Acad. Sci. USA.* 69:3561–3566.

Oliva, M., V. De Pinto, P. Barsanti, and C. Caggese. 2002. A genetic analysis of the porin gene encoding a voltage-dependent anion channel protein in Drosophila melanogaster. *Mol. Genet. Genomics.* 267:746–756.

Rapizzi, E., P. Pinton, G. Szabadkai, M. R. Wieckowski, G. Vandecasteele, G. Baird, R. A. Tuft, K. E. Fogarty, and R. Rizzuto. 2002. Recombinant expression of the voltage-dependent anion channel enhances the transfer of Ca2+ microdomains to mitochondria. *J. Cell Biol.* 159:613–624.

Rostovtseva, T. K., and M. Colombini. 1996. ATP flux is controlled by a voltage-gated channel from the mitochondrial outer membrane. *J. Biol. Chem.* 271:28006–28008.

Rostovtseva, T. K., A. Komarov, S. M. Bezrukov, and M. Colombini. 2002. Dynamics of nucleotides in VDAC channels: structure-specific noise generation. *Biophys. J.* 82:193–205.

Rubin, G. M., L. Hong, P. Brokstein, M. Evans-Holm, E. Frise, M. Stapleton, and D. A. Harvey. 2000. A Drosophila complementary DNA resource. *Science.* 287:2222–2224.

Ryerse, J., E. Blachly-Dyson, M. Forte, and B. Nagel. 1997. Cloning and molecular characterization of a voltage-dependent anion-selective channel (VDAC) from Drosophila melanogaster. *Biochim. Biophys. Acta.* 1327:204–212.

Sampson, M. J., W. K. Decker, A. L. Beaudet, W. Ruitenbeek, D. Armstrong, M. J. Hicks, and W. J. Craigen. 2001. Immotile sperm and infertility in mice lacking mitochondrial voltage-dependent anion channel type 3. *J. Biol. Chem.* 276:39206–39212.

Sampson, M. J., R. S. Lovell, and W. J. Craigen. 1997. The murine voltage-dependent anion channel gene family. Conserved structure and function. *J. Biol. Chem.* 272:18966–18973.

Sampson, M. J., R. S. Lovell, D. B. Davison, and W. J. Craigen. 1996. A novel mouse mitochondrial voltage-dependent anion channel gene localizes to chromosome 8. *Genomics.* 36:192–196.

Song, J., C. Midson, E. Blachly-Dyson, M. Forte, and M. Colombini. 1998a. The topology of VDAC as probed by biotin modification. *J. Biol. Chem.* 273:24406–24413.

Song, J., C. Midson, E. Blachly-Dyson, M. Forte, and M. Colombini. 1998b. The sensor regions of VDAC are translocated from within the membrane to the surface during the gating processes. *Biophys. J.* 74: 2926–2944.

The-FlyBase-Consortium. 2003. The FlyBase database of the Drosophila genome projects and community literature. *Nucleic Acids Res.* 31:172–175.

Thomas, L., E. Blachly-Dyson, M. Colombini, and M. Forte. 1993. Mapping of residues forming the voltage sensor of the voltage-dependent anion-selective channel. *Proc. Natl. Acad. Sci. USA.* 90:5446–5449.

Vander Heiden, M. G., N. S. Chandel, X. X. Li, P. T. Schumacker, M. Colombini, and C. B. Thompson. 2000. Outer mitochondrial membrane permeability can regulate coupled respiration and cell survival. *Proc. Natl. Acad. Sci. USA.* 97:4666–4671.

Vander Heiden, M. G., X. X. Li, E. Gottleib, R. B. Hill, C. B. Thompson, and M. Colombini. 2001. Bcl-x_L promotes the open configuration of VDAC and metabolite passage through the mitochondrial outer membrane. *J. Biol. Chem.* 276:19414–19419.

Weeber, E. J., M. Levy, M. J. Sampson, K. Anflous, D. L. Armstrong, S. E. Brown, J. D. Sweatt, and W. J. Craigen. 2002. The role of mitochondrial porins and the permeability transition pore in learning and synaptic plasticity. *J. Biol. Chem.* 277:18891–18897.

Xu, X., W. Decker, M. J. Sampson, W. J. Craigen, and M. Colombini. 1999. Mouse VDAC isoforms expressed in yeast: channel properties and their roles in mitochondrial outer membrane permeability. *J. Membr. Biol.* 170:89–102.